

Damped frequencies of precast modular steel-concrete composite railway track slabs

Sakdirat Kaewunruen^{*1} and Stephen Kimindiri Kimani^{2a}

¹Birmingham Centre for Railway Research and Education, School of Engineering, University of Birmingham, Birmingham B15 2TT UK

²Department of Civil Engineering, School of Engineering, University of Birmingham, Birmingham B15 2TT UK

(Received March 27, 2017, Revised July 15, 2017, Accepted August 04, 2017)

Abstract. This paper presents unprecedented damped oscillation behaviours of a precast steel-concrete composite slab panel for track support. The steel-concrete composite slab track is an innovative slab track, a form of ballastless track which is becoming increasingly attractive to asset owners as they seek to reduce lifecycle costs and deal with increasing rail traffic speeds. The slender nature of the slab panel due to its reduced depth of construction makes it susceptible to vibration problems. The aim of the study is driven by the need to address the limited research available to date on the dynamic behaviour of steel-concrete composite slab panels for track support. Free vibration analysis of the track slab has been carried out using ABAQUS. Both undamped and damped eigenfrequencies and eigenmodes have been extracted using the Lancsoz method. The fundamental natural frequencies of the slab panel have been identified together with corresponding mode shapes. To investigate the sensitivity of the natural frequencies and mode shapes, parametric studies have been established, considering concrete strength and mass and steel's modulus of elasticity. This study is the world first to observe crossover phenomena that result in the inversion of the natural orders without interaction. It also reveals that replacement of the steel with aluminium or carbon fibre sheeting can only marginally reduce the natural frequencies of the slab panel.

Keywords: free vibration; steel-concrete composite; ballastless track; slab panel track; natural frequency; natural mode; mass; stiffness; crossover; veering

1. Introduction

This paper focuses on the unprecedented study undertaken on the damped free vibrations of a precast steel-concrete composite slab panel for track support developed by Griffin (2013) and it is a companion to Kimani and Kaewunruen (2017). The slab panel track is a form of ballastless track system. An increase in train speed and axle loading and problems facing conventional ballasted track systems in the last 40 years gave rise to ballastless track systems (Michas 2012). The problems associated with ballasted track systems are; the increased speeds and daily movements of high-speed services has resulted in significant degradation of the systems (Matias 2015); movements of the system during loading translates to energy leading to degradation of the ballast and track quality hence increased need for maintenance (Bezin and Farrington 2010); Low design life compared to other systems (Britpave 2016) and scarcity of high-quality ballast material (Peng *et al.* 2012). Though not an issue limited to ballasted tracks only, susceptibility of timber sleepers to both biological and mechanical deterioration is a problem with these systems (Manalo *et al.* 2010). In addition to overcoming the demerits of a ballasted track system

described above, other justifications for a ballastless track are; need for track which is accessible to road vehicles; reduced track noise and vibration requirements; avoid environmental pollution by release of dust from ballast; reduced height of construction and reduced maintenance requirements and therefore higher track availability (Esveld 1997, Tuler and Kaewunruen 2017). According to Robertson *et al.* (2015), growing economic pressure is pushing railway asset owners worldwide to reduce their life cycle costs hence ballastless track systems are becoming more attractive compared to ballasted tracks. In addition, increasing speeds and need for large operational windows to meet the growing interest in mixed passenger-freight lines make a ballastless track attractive over ballasted tracks.

The aim of the study is to determine the free vibration of the precast steel-concrete composite slab panel for track support by using finite element (FE) method. Based on the literature review undertaken for the study, limited information is currently available on the vibration behaviour of steel-concrete composite slab panel for track support. This study aims to bridge that gap and provide the base study on which future research could be undertaken. Steel-concrete composite slab panel for track support is currently being considered in the replacement of ageing deck elements in steel-girder railway bridges as it provides slim deck construction offering savings in dead load and improved durability (Griffin *et al.* 2014, 2015, Setsobhonkul *et al.* 2017). The slender construction and the one-way spanning nature of the panel make it vulnerable to vibration problems (De Silva and Thambiratnam 2011,

*Corresponding author, Senior Lecturer,
E-mail: s.kaewunruen@bham.ac.uk

^aFormerly Masters Student,
E-mail: kimindiri2000@yahoo.com

Kaewunruen and Remennikov 2007, 2016).

The technology of the steel-concrete composite slab panel track has developed as an improvement to concrete slab tracks. This type of slab track is much suited for the replacement of deck and track elements in existing railway bridges (Griffin 2013). According to Choi *et al.* (2010) timber track steel plate girder bridges have been in use for many years now, and over time, the bridges have deteriorated due to corrosion, abrasion, cracking and deformation of members. This has led to a decline in structural safety and durability. Growth in passenger numbers and freights, changes in design loads and environmental conditions have all exacerbated the condition of these bridges. Choi *et al.* (2010) have identified the following major problems associated with timber tracks on steel plate girder bridges:

- Long-term degradation of impact absorption due to vulnerability to train impact loads.
- Frequent need of replacement of track components.
- More than necessary maintenance effort due to the high proportion (50% - 60%) of maintenance work being replacement of the tie plates and sleepers only.
- Track insulation resistance elements degradation due to exposure to rain.

Replacement of the timber track on these bridges needs developing an innovative type of ballastless track to cope with the following construction constraints as identified by Choi *et al.* (2010) and Griffin *et al.* (2014); maintaining same track levels before and after track replacement; narrow windows for construction for operational tracks; limitations in the steel girder strength; low clearances for platforms and tracks and inadequate widths at structures. A number of researchers have developed solutions to cope with the above challenges. Choi *et al.* (2010) developed a precast steel-concrete composite slab panel (PSP) track with the objective of improving long-term workability and durability of the existing bridges in order to enhance performance of railway lines. Griffin (2013) and Griffin *et al.* (2014, 2015) researched on a theoretical design solution of a precast steel-concrete composite slab panel to replace the existing timber track on the Sydney Harbour Bridge as shown in Fig. 1.

Other types of steel-concrete composite slab track that have been developed include the steel girder-precast concrete slab track developed by Sugimoto *et al.* (2013). In the field of highway bridges, Kim and Jeong (2006, 2009 and 2010) proposed use of a profiled steel sheeting with perfobond ribs as participating formwork for box girder composite deck construction. Relevant research work to composite slab decks was undertaken by Shim *et al.* (2001) to investigate the headed shear studs shear capacity in composite precast concrete slab-steel girders for road bridges. The steel-concrete composite precast slab panel developed by Griffin (2013) comprised of a minimum 0.18m deep composite slab with a 1mm thick BONDEK II profiled steel sheeting. The overall length of the slab was 3.237 m. The panel sections within 0.616 m from both ends were locally thickened to 0.23 m deep to resist hogging moments due to derailment loads. The panel acts

compositely with the supporting pair of steel girders and spans 2.205 m measured from the centre lines of the steel girders. Composite action between the panel and the supporting steel girders was achieved via two rows x 3 columns of headed shear studs welded to the top flanges through the profiled steel sheeting at the flange locations. Shear reinforcement was provided in form of 10 mm diameter link bars as follows; 12 no. links at 0.13 m centre-to-centre spacing were provided for the 0.18 m deep section and 4 no. links at 0.1 m centre-to-centre spacing were provided for the 0.23 m deep section of the panel. Details of the composite precast slab are shown on Fig. 1 and the material properties are summarised in Table 1 below.

2. Previous research

According to Smith *et al.* (2009), the solutions to the vibration problems of continuous systems can be generally found using integration of continuous functions. However, according to Chopra (2011), due to the infinite number of degrees of freedoms for continuous systems, their analysis is not feasible for practical structures. Due to the simplicity of the matrices methods used for MDOF systems, techniques are available that discretize one-dimensional continuous systems (e.g., beam in transverse vibration only) to allow their solutions to be found using matrices methods. As a result, a system of ordinary differential equations, as many as the DOFs required, replaces the governing partial differential equation of the one-dimensional continuous system.

Table 1 Precast steel-concrete composite slab panel materials properties

Material	Properties
Concrete	28 days cube strength, f'_c : 50 N/mm
	Short-term modulus of elasticity: 34652 N/mm ²
	Poison ratio: 0.2
	Density: 2400 Kg/m ³
Profiled steel sheeting (High Tensile Steel Bondek II profile manufactured by BHP Building Products)	Yield stress: 550 N/mm ²
	Thickness: 1.0 mm
	Modulus of Elasticity: 200000 N/mm ²
Tensile and shear steel reinforcement (D500N grade)	Poison ratio: 0.3
	Yield stress: 500 N/mm ²
	Modulus of Elasticity: 200000 N/mm ²
Shear studs	Poison ratio: 0.3
	Yield stress: 420 N/mm ²
	Modulus of Elasticity: 200000 N/mm ²
Supporting steel girders	Poison ratio: 0.3
	Yield stress: 300 N/mm ²
	Modulus of Elasticity: 200000 N/mm ²
	Poison ratio: 0.3

$$\left(\mu^2[M] + \mu[C] + [K]\right) \{\phi\} = 0 \quad (1)$$

where $[M]$ is the symmetric and positive definite mass matrix; $[C]$ is the damping matrix; $[K]$ is the stiffness matrix; μ is the eigenvalue and $\{\phi\}$ is the eigenvector – the mode of vibration.

The solution to Eq. (1) will have complex eigenvalues and eigenvectors. To obtain a solution with real squared eigenvalues μ^2 , and real eigenvectors only, equation 2-1 can be symmetrized by assuming that $[K]$ is symmetric and by neglecting $[C]$ during the eigenvalue extraction. By assuming further that $[K]$ is positive semi-definite, then μ becomes an imaginary eigenvalue $\mu = iw$ where w is the circular frequency. The eigenproblem can therefore be expressed as

$$\left(-w^2[M] + [K]\right) \{\phi\} = 0 \quad (2)$$

As mentioned earlier, Choi *et al.* (2010), Griffin (2013), Sugimoto *et al.* (2013); Kim and Jeong (2006, 2009, 2010) and Shim *et al.* (2001) have all developed solutions for steel-concrete composite slab panel deck, however, none of the researchers have undertaken work on the dynamic behaviour of the composite slab decks proposed. Choi *et al.* (2010) have investigated the dynamic behaviour of a steel plate girder for a bridge specimen comprising of a steel-concrete composite precast slab panel track deck simply supported on a pair of steel plate girders. The reasonable conclusion made is that limited literature is currently available on the free vibration of the steel-concrete composite slab panel for track support. The steel-concrete composite technology is however quite common in the building sector for the construction of profiled steel decking-concrete composite floors. Several researchers, among them De Silva and Thambiratnam (2011), Feldmann *et al.* (2009), Venghiac and D'Mello (2010), El-Dardiry and Ji (2006) and Mello *et al.* (2008) have investigated the dynamic behaviour of profiled steel sheeting-concrete composite floor slabs and therefore relevant aspects of their works to the free vibration of the steel-concrete composite slab panel were reviewed for this study.

Choi *et al.* (2010) investigated the dynamic behaviour of a precast slab panel (PSP) track girder by undertaking dynamic testing of a full-scale specimen and also undertaking a FE analysis of a 3-dimensional model of the PSP and supporting steel girders. Though the result of their work provided the natural frequency of the 1st mode for the steel plate girder only, which is not relevant to this study, their approach to the FE analysis modelling of the PSP is important. A 3D FE model of the test specimen was developed in LUSAS and MIDAS FE computer packages by using the 3D solid elements for the concrete slab and frame elements for the rails. Connections between the rails and PSP slab, and those between the PSP and the steel plate girders were modelled as elastic spring elements. The steel plate girders and bracings were modelled as shell elements. It is not clear how Choi *et al.* (2010) modelled the steel plate component in the composite PSP slab and the steel reinforcement in the slab as no information is provided on these aspects. As Choi *et al.* (2010) investigation was

focused on the dynamic behaviour of the steel plate girder only, information on the natural frequencies and mode shapes of the PSP, which would have been of tremendous relevance to this study, is lacking. Griffin (2013) on the other hand undertook a detailed FE analysis modelling approach, using ABAQUS/Standard, to model the steel-concrete composite slab used in his study. The concrete slab, profiled steel sheeting, shear studs and the supporting steel girder were all modelled as 3-dimensional solid elements (C3D8R hourglass control) whilst the steel reinforcement was modelled as 3-dimensional truss elements (T3DR). Careful consideration was taken in defining contacts and interactions between the various components of the 3D FE model as these had a direct influence on the general response of the individual components and the whole structural system. Griffin (2013) 3D FE model is described in more detail in section 4 of this paper.

De Silva and Thambiratnam (2011) investigated the vibration characteristics of a profiled steel sheeting-concrete composite multi-panel floor slab using FE analysis in ABAQUS/Standard. The floor system comprised of a 0.15 m deep composite floor slab with 1mm thick profiled steel sheeting which is similar in construction to the precast composite slab panel used in Griffin (2013) study. However, the FE modelling approach adopted by De Silva and Thambiratnam (2011) differed from Griffin (2013) as the floor slab was modelled as follows; the concrete slab was modelled as 3D solid elements (3S6); the profiled steel sheeting was modelled as shell elements (S4R5) and the interface between the steel sheeting and the concrete slab was modelled as full interaction with no slip between the two materials. According to Dassault (2012), for FE modelling incorporating contacts, accuracy issues may arise when using shell elements compared to solid elements. Unlike Griffin (2013) panel which is a single panel supported on a pair of steel girders, De Silva and Thambiratnam (2011) multi-panels were part of a larger floor system comprising of primary and secondary steel beams and columns. This would indicate that the natural frequencies and mode shapes of the two systems would be quite dissimilar due to the difference in boundary conditions, floor mass activated in each mode and stiffness of the floor systems. Nonetheless, the material damping of the bare profiled steel sheeting-concrete composite slabs would be similar. According to De Silva and Thambiratnam (2011), damping for steel-concrete composite floor system is reported to be between 1.5% - 1.8%. However, heel-drop tests performed by De Silva and Thambiratnam (2011) on steel-concrete composite slab panels showed damping levels of 1.75% - 2.0%. According to Feldmann *et al.* (2009), the material damping ratios for steel, concrete and steel-concrete composite are given as 1%, 2% and 1% respectively. Since the damping ratios are assigned to the respective members of a composite.

El-Dardiry and Ji (2006) carried out work on the modelling of dynamic behaviour of profiled steel sheeting-concrete slab floors using FE analysis in LUSAS FE program. In addition, they carried out parametric studies to investigate the effect of the profiled steel sheeting contribution, among other parameters, to the natural

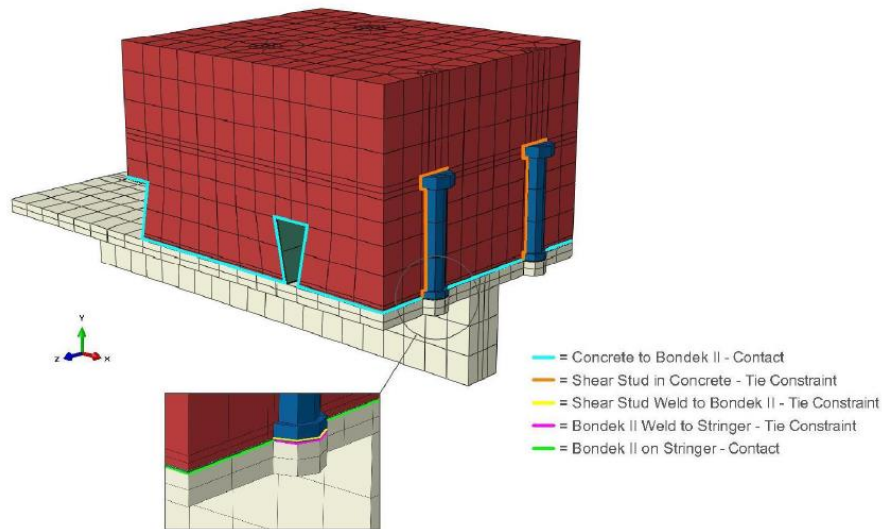


Fig. 2 FE Model of a modular panel for track slabs

frequency of the floor slab system. El-Dardiry and Ji (2006) floor system comprised of a 0.13m deep composite slab with 0.9mm thick profiled steel sheeting and this is similar in construction to the slabs used by Griffin (2013) and De Silva and Thambiratnam (2011) in their studies. El-Dardiry and Ji (2006) modelled their concrete slab as 3D solid elements and the profiled steel sheeting as thin shell elements which is similar to the modelling approach adopted by De Silva and Thambiratnam (2011). It is not clear, however, how El-Dardiry and Ji (2006) modelled the contact between the concrete slab and the profiled steel sheeting as this information is not given in their work. El-Dardiry and Ji (2006) study found out that removing the profiled steel sheeting from the composite slab reduced the fundamental natural frequency by approximately 5%. This was attributed to the decrease in the stiffness of the composite slab (location of sheeting at extreme fibre and elastic stiffness of steel approximately 6-7 times the elastic stiffness of the concrete) with slight reduction in the mass of the system (mass of 0.9mm thick sheeting negligible relative to mass of concrete).

Venghiac and D'Mello (2010) undertook parametric studies to investigate the effect on the fundamental natural frequency for composite slab panels of varying width:length aspect ratios due to the following influences; thickness of slab and grade of concrete. The floor slab used in their study comprised of a 0.375 m deep composite slab with 1.22 mm thick profiled steel sheeting (deep profile). The composite slab was modelled as an orthotropic plate in Autodesk Robot Structural Analysis FE program. The parametric studies showed that for a given aspect ratio of the slab panel, increasing the grade of the concrete led to an increase in the fundamental natural frequency of the composite slab. This could be attributed to the increase in stiffness of the composite slab with no increase in mass of the system.

Based on this critical review, it can be found that the undamped and damped free vibration behaviors of steel-concrete composite panels have not been fully investigated.

In fact, the track slabs often expand longitudinally and it is critically important to investigate fully the dynamic behaviors in three dimensions, especially the coupling modes.

3. Finite element modelling and its validation

A finite element (FE) model has been developed to represent the modular track slabs as shown in Fig. 2. The FE model has been validated using theoretical studies and sensitivity analyses (Mirza *et al.* 2016).

Material properties

Griffin (2013) modelled the concrete and steel in the slab panel as elastic-plastic materials in his study. The concrete and steel properties for the elastic range are as shown in Table 1 of this paper. The plastic properties are not described herein as this are outside the scope of this study.

Element type and mesh

The concrete slab, profiled steel sheeting, shear studs and supporting steel girders were modelled as solid, 3dimensional eight node (C3D8R) elements with hourglass control. A description of each of these initials is provided below (Griffin 2013);

- | | |
|----|---|
| C | Solid continuous family |
| 3D | 3 degrees of translational degrees of freedom at each node of the element |
| 8 | The number of nodes of the element at which the degrees of freedom are calculated |
| R | Reduced integration which is effective in reducing analysis time by only calculating the degrees of freedoms at optimum nodes |

Table 2 Contacts and interactions between composite slab panel materials

Interface	Interface Type	Master Surface	Slave Surface
Reinforcing steel in concrete	Embedded	Reinforcing steel	Concrete
Concrete to Bondek II	Surface to Surface Contact	Bondek II	Concrete
Shear stud in concrete	Tie constraint	Shear stud	Concrete
Shear stud weld to Bondek II	Tie constraint	Bondek II	Shear stud
Bondek II weld to stringer	Tie constraint	Bondek II	Stringer
Bondek II on stringer	Surface to Surface Contact	Bondek II	Stringer

Table 3 Concrete strength and dynamic modulus of elasticity used in the parametric study

	Concrete strength, $f_{ck,cube}$ (N/mm ²)							
	37	45	50	60	75	95	105	115*
E_{cm} (KN/mm ²)	33	34	35	37	39	42	44	45*
E_{dyn} (KN/mm ²)	36.3	37.4	38.5	40.7	42.9	46.2	48.4	49.5

* Reasonable values assumed for the study

The demerit of reduced integration is that it can lead to ‘hourglassing’ which is the phenomenon of errors being propagated through the model due to zero stresses and strains being introduced at other nodes. Hourglass control is therefore introduced in order to correct these zero stresses and strains and reduce the errors arising from such phenomenon (Griffin 2013). The steel reinforcement was modelled as 3-dimensional 2 node truss (T3DR) elements. The ‘T’ stands for truss family. The truss elements are tension and compression only members and were modelled embedded in the concrete (Griffin 2013).

Contacts and interactions

Table 2 and Fig. 5 below adopted from Griffin (2013) summarise the contacts and interactions between the composite slab panel materials. It is worth noting that the contact between the concrete and the profiled steel sheeting was modelled as a surface-to-surface contact with finite sliding, hard contact in the normal direction and a coefficient of friction of 0.5 in the tangential direction (Griffin 2013). One of the recommendations of this study is to evaluate the sensitivity of the natural frequencies of the slab panel to the variation of this friction coefficient.

Boundary conditions

The cut edges of the supporting steel girders were assigned encastre boundary conditions i.e., fixity in the 3 degrees of translational freedom and fixity in the 3 degrees of rotational freedom.

Aspects amended to suit free vibration analysis

The materials were assigned mass properties as follows; concrete was assigned a mass of 2400 Kg/m³ in accordance with table 1-1 and steel was assigned a mass of 7850Kg/m³

in accordance with BS EN 1991-1-1:2002 (British Standards Institution, 2002) as Griffin (2013) had not proposed any value for steel.

Material properties adopted for the parametric studies

The rationale behind the values adopted for the material properties for the parametric studies was as follows.

The range of concrete strength values was adopted from BS EN 1992-1-1:2004 in Table 3 (British Standards Institution, 2004). The dynamic elastic modulus, E_{dyn} , was determined by factoring the short-term modulus of elasticity, E_{cm} , of the concrete by a value of 1.1 as recommended by Feldmann *et al.* (2009). These values are summarised in Table 3. The range of the concrete mass values was adopted from BS EN 206-1:2000 (British Standards Institution, 2000) for normal weight concrete. These were 2000 Kg/m³; 2200 Kg/m³; 2400 Kg/m³ and 2600 Kg/m³. Additional arbitrary values of 1000 Kg/m³ and 1500 Kg/m³ were considered to account for emerging trends in using high strength light-weight concrete in structures.

The range of the steel modulus of elasticity, E_s was chosen based on the varying values of E_s provided by British Standards Institution (2005, 1994, 1995) i.e., BS EN 1993-1-1 gives a value of 210 kN/mm²; BS 5950 part 4 and 6 give values of 205 kN/mm² and 210 kN/mm² respectively and the value of 200 kN/mm² used by Griffin (2013). Additional arbitrary values of 50 kN/mm², 100 kN/mm² and 150 kN/mm² were considered to account for loss of stiffness from corrosion and fire damage. A range of 50 kN/mm² to 215 kN/mm² was therefore adopted for the parametric analysis.

Values for the material properties adopted for the aluminium and high modulus carbon fibre (HMCF), used as alternative materials to steel sheeting, are summarised in

Table 4 Concrete strength and dynamic modulus of elasticity used in the parametric study

Material	Properties
Aluminium	Yield stress: 290 N/mm ²
	Modulus of elasticity: 78500 N/mm ²
	Poison ratio: 0.325
	Density: 2750 Kg/m ³
High modulus carbon fibre	Yield stress (tensile/compressive): 350/150 N/mm ²
	Modulus of elasticity(0° and 90°): 85000 N/mm ²
	Density: 1600 Kg/m

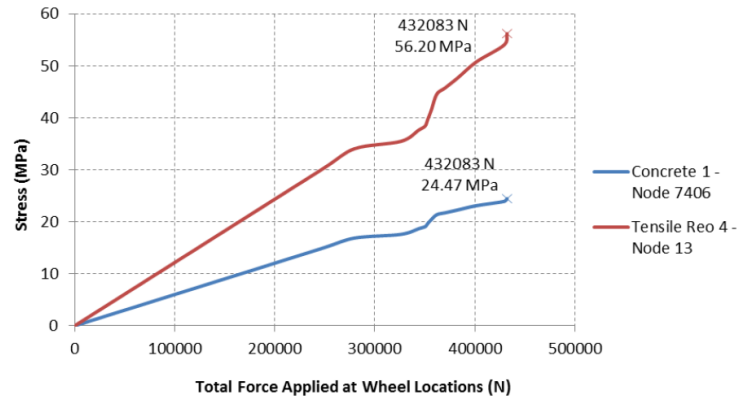


Fig. 3 Model stress-load relationship, node 7406 and node 13 by Griffin (2014)

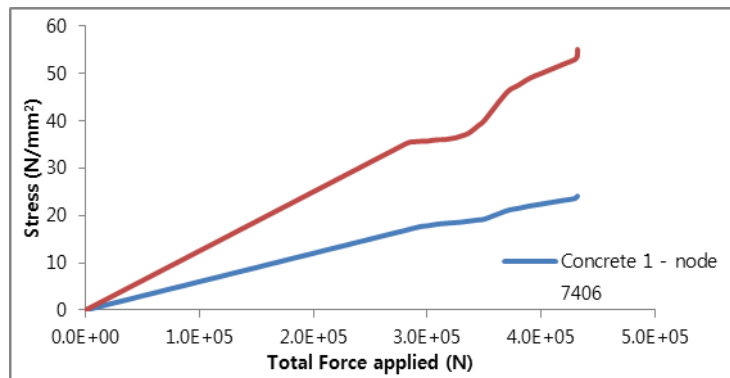


Fig. 4 Model validation stress-load relationship, node 7406 and node 13 in this study

Table 4. The aluminium properties were an arbitrary extract from Tindall (2008) Table 1 whilst the HMCf were arbitrarily adopted from ACP Composites (2016).

Damping ratio

The damping ratio range of 1% - 5% used in the parametric study was considered reasonable for the steel-concrete composite slab panel based on the literature review.

Composite damping ratio

Dassault (2012) method of computing the composite damping ratio for composite structure is expressed in Eq. (3) below

$$\xi_{\alpha} = \frac{1}{m_{\alpha}} \phi_{\alpha}^N \left(\sum \xi_{\alpha} M_{\alpha}^{NM} \right) \phi_{\alpha}^M \tag{3}$$

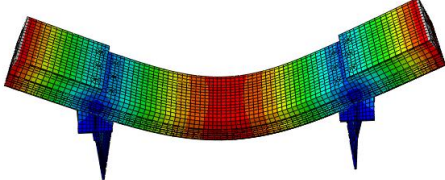
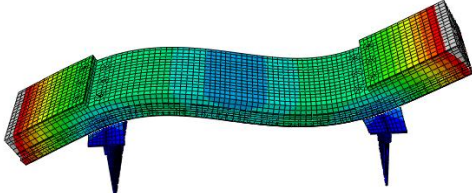
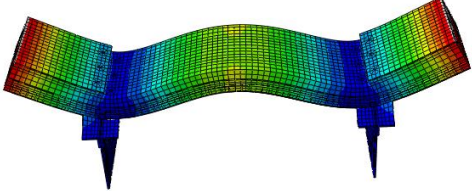
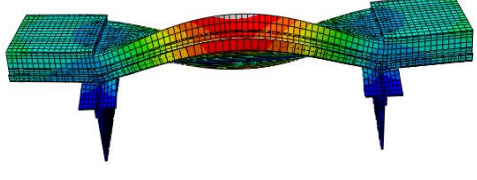
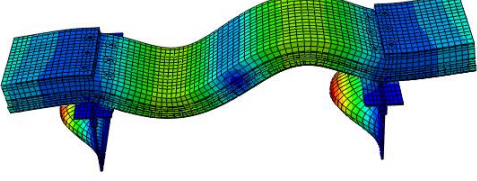
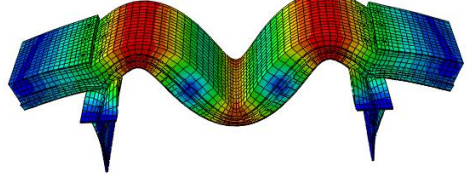
Where ξ_{α} is the composite damping ratio; m_{α} is the

generalised mass; ξ_{α} is the material damping ratio for material a; ϕ_{α} is the eigenvector for the α mode; α is the mode and N and M are the degrees of freedom of the model.

Validation of FE model

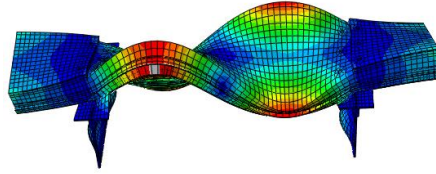
An abbreviated validation was carried out by undertaking a comparison of Griffin (2013) derailment loading results for selected nodes with results from similar

Table 5 Composite damping ratio (ξ_α) and associated modes of the slab panel (based on material damping ratios of 1% for steel and 2% for concrete)

Mode of vibration	Composite damping ratio (%) and corresponding modeshapes
1 st mode - transverse bending	 <p data-bbox="986 600 1050 627">1.9011</p>
2 nd mode- transverse bending	 <p data-bbox="986 846 1050 873">1.9145</p>
3 rd mode-transverse bending	 <p data-bbox="986 1081 1050 1108">1.9099</p>
4 th mode-torsion	 <p data-bbox="986 1305 1050 1332">1.8989</p>
5 th mode-transverse bending	 <p data-bbox="986 1552 1050 1579">1.7896</p>
6 th mode –transverse bending	 <p data-bbox="986 1776 1050 1803">1.8821</p>

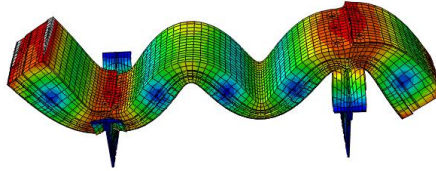
Continued-

7th mode-torsion



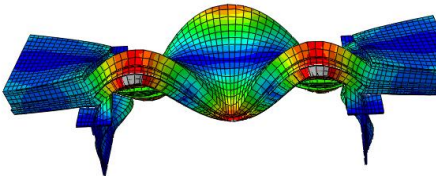
1.8821

8th mode transverse bending



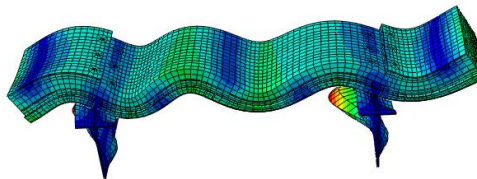
1.8094

9th mode- torsion



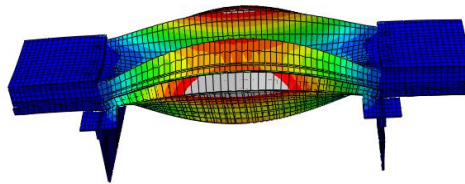
1.8483

10th mode-transverse bending



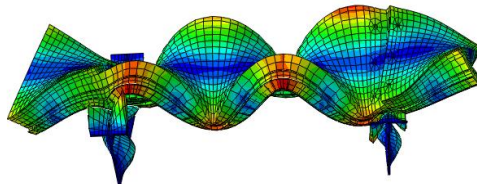
1.7671

11th mode- bi-directional bending



1.8828

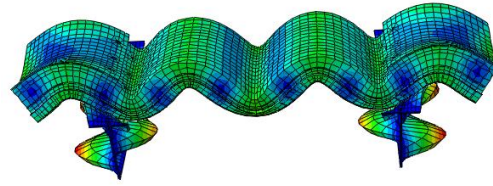
12th mode-torsion



1.8135

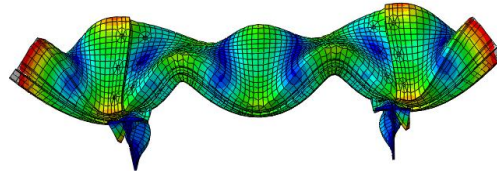
Continued-

13th mode-transverse
bending



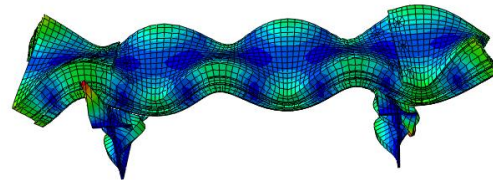
1.6600

14th mode-torsion



1.8421

15th mode-torsion



1.7422

derailment loading. Figs. 3 and 4 show the load-stress relationships of the structure carried out by Griffin (2014) and by the authors in this study, respectively. The 3-dimensional FE model is deemed to be in very good agreement as the two results were within 5% variation of each other i.e., 55.1 N/mm² for node 7406 and 24.2 N/mm² for node 13.

4. Free vibration analyses

4.3 Damped system natural frequencies and mode shapes

4.3.1 Composite damping ratio

Table 5 shows the computed ABAQUS/Standard computed composite damping ratios for the modeshapes of the slab panel based on material damping ratios of 1% for steel and 2% for concrete.

4.3.2 Parametric study on the variation of damping ratio

The damped natural frequencies and associated modes for the computed composite damping, and uniform damping ratios of 1%; 2%; 3%; 4% and 5% are shown in Table 7.

5. Discussions

5.1 Natural frequencies

The fundamental undamped natural frequency of the slab panel was found to be 2.5981Hz. The fundamental damped natural frequency was determined as 2.5976Hz based on the ABAQUS/Standard computed composite damping ratio of 1.901%. This ratio was calculated from material damping ratios of 1% for steel and 2% for concrete as given by Feldmann et al (2009). It can be clearly seen that the difference between the two values of 0.018% is negligible and this agrees with Chopra (2011) assertion that the effects of damping on the natural frequency of most structures are negligible as their damping ratios are below 20%.

From the literature review, previous work on dynamic behaviour of a slab panel deck similar to Griffin (2013) was not available. A direct comparison of the results with previous work was therefore not possible. Nonetheless, the fundamental natural frequency of the slab panel was compared with the results of De Silva and Thambiratnam (2011) and, as expected, the value was lower relative to the natural frequency of 4.0Hz for the 4-panel profiled steel sheeting-concrete slab composite floor slab in their study.

This could be attributed to the relatively higher stiffness of the primary beams-secondary beams-composite floor system compared with Griffin (2013) slab panel.

Table 7 Damped natural frequencies of slab panel at various damping ratios (Hz)

Mode of vibration	Composite damping ratio	Material damping ratio				
		Uniform damping ratio				
		1%	2%	3%	4%	5%
1 st mode - transverse bending	2.5976	2.5979	2.5976	2.5969	2.5960	2.5948
2 nd mode- transverse bending	4.1642	4.1647	4.1641	4.1631	4.1616	4.1597
3 rd mode-transverse bending	6.8787	6.8796	6.8786	6.8769	6.8745	6.8714
4 th mode-torsion	9.7104	9.7117	9.7102	9.7078	9.7044	9.7000
5 th mode-transverse bending	12.3689	12.3703	12.3684	12.3653	12.3610	12.3554
6 th mode –transverse bending	20.8452	20.8477	20.8445	20.8393	20.8320	20.8226
7 th mode-torsion	21.1302	21.1328	21.1297	21.1244	21.1170	21.1075
8 th mode transverse bending	27.1463	27.1493	27.1453	27.1385	27.1290	27.1167
9 th mode- torsion	32.2957	32.2996	32.2947	32.2867	32.2753	32.2608
10 th mode-transverse bending	37.1311	37.1350	37.1295	37.1202	37.1072	37.0904
11 th mode- bi-directional bending	38.8293	38.8343	38.8284	38.8187	38.8051	38.7876
12 th mode-torsion	42.3561	42.3610	42.3546	42.3440	42.3292	42.3101
13 th mode-transverse bending	46.0209	46.0249	46.0180	46.0065	45.9904	45.9696
14 th mode-torsion	46.7430	46.7486	46.7415	46.7299	46.7135	46.6924
15 th mode-torsion	51.2688	51.2740	51.2663	51.2535	51.2356	51.2125

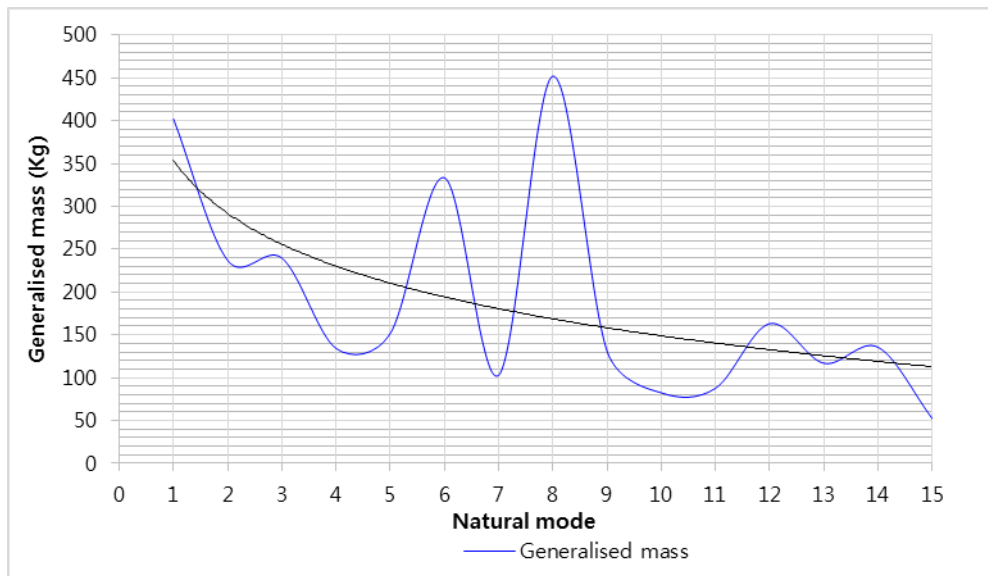


Fig. 10 Variation of system generalised mass with increasing modes

5.2 Changes in natural frequencies

Fig. 5 shows an increase of the natural frequencies with increasing modes of vibration for the slab panel. The slab panel, which is a continuous system was discretized and analysed as a MDOF system. From Eq. (5) below adopted from Chopra (2011), which is the formal non-trivial solution of the matrix eigenvalue problem of an undamped MDOF system, it can be seen that equating the scalar w_n^2 to the stiffness-mass ratio, \mathbf{k}/\mathbf{m} , means that an increase in the natural frequencies of the slab panel is attributed to the

increase in this ratio with each increasing mode of vibration of the system.

$$\det[\mathbf{k} - w_n^2 \mathbf{m}] \quad (5)$$

As was demonstrated by the parametric studies, varying the \mathbf{k} and \mathbf{m} of the slab panel resulted in either a decrease or increase of the natural frequencies. Fig. 10 shows the decreasing trend in the generalised mass from mode to mode which goes to show the stiffness-mass ratio increases with increasing modes of vibration.

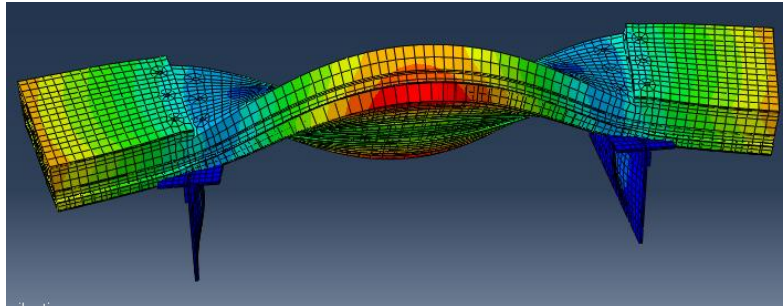


Fig. 11 Coupled torsion and bending about minor axis mode of vibration

5.3 Dynamic mode shapes

15 distinctive mode shapes were identified as the natural modes of vibration from the first 500 eigenmodes extracted by the Lanczos eigensolver in ABAQUS/Standard. As described in the methodology of this study, higher order eigenmodes (above the 52nd eigenmode) were immediately removed as their mode shapes were not visually distinctive since these were associated with low amplitude vibrations of the concrete slab. Eigenmodes which were dominated by the vibration of the steel support girders (buckling of the webs and flanges) were filtered out as well as the vibration of the support girders was not part of the study. Coupled eigenmodes were removed as these could not be described as pure modes of vibration of the slab panel. For example, the 8th eigenmode extracted from the Lanczos eigensolver, shown below in Fig. 11, was observed to both twist and bend the slab panel about the minor axis. In addition, eigenmodes with very close eigenfrequencies were identified and the non-dominant ones removed to ensure that only one natural mode was associated with that natural frequency. The fundamental natural mode shape was identified as transverse bending of the slab panel. From Tables 5 and 6, it can be seen that the first 15 natural mode shapes of the slab panel are dominated by the transverse bending (8 modes) and torsion mode shapes (6 modes). This is expected due to the slender and one-way spanning nature of the slab panel. The only other mode shape identified was the bi-directional bending of the slab panel which could be attributed to the reduced depth of the slab in the longitudinal direction due to the profile of the steel sheeting.

A correlation of the natural frequencies of the slab panel with typical rail frequency ranges was made as shown in Fig. 5. The first 7 natural frequencies can be seen to fall within the range of low speed rail frequencies hence resonance damage to the slab panel from low speed rail vibrations is most likely to result from transverse bending of the slab panel. Likewise resonance damage to the slab panel from semi-high speed and high speed rail vibrations will likely result from transverse bending or torsion of the slab panel as these modes dominate these two ranges.

5.4 Composite damping ratio

Fig. 12 below shows the variation of the composite damping ratio with increasing modes. It can be seen that the composite damping ratio is very close the uniform 2% damping ratio for the 15 natural modes (average variance of 9%). The fundamental damped natural frequency calculated from the composite damping ratio was found to be the same as the fundamental damped natural frequency calculated from the 2% uniform damping ratio. From Table 7, it can be seen that the damped natural frequencies for both the composite and uniform 2% damping ratios for the natural modes are very close and the difference is marginal. This goes to show that for the concrete dominated composite slab panel, a uniform damping ratio based on the concrete material could be deemed representative of the composite damping nature of the slab panel.

As described in the FE modelling section of this paper, the composite damping ratio was computed based on a mass weighting i.e., the steel or concrete part of the mass matrix as a fraction of the generalised mass matrix for each specific mode. Limitations of this method by Dassault (2012) were identified as follows:

- A sensitivity check on the computation of the composite damping showed that for a 2% material damping ratio for both steel and concrete, the computed composite damping ratio was found to be 2% for all the modes. According to Dassault (2012) the parts of the mass matrix made up of the steel and the concrete change from mode to mode. The eigenvector and the generalised mass of the system change as well from mode to mode. On this basis, the computed composite damping ratio for a 2% material damping ratio for both steel and concrete cannot be 2% for all the modes.
- Fig. 13 below shows the computed damping ratio for the first 49 eigenmodes extracted from the Lanczos eigensolver in ABAQUS/Standard. It can be seen that the modes dominated by the vibration of the supporting steel girders were observed to have spikes (computed composite damping ratios close to 1%) due to the inclusion of the supporting girders' mass in the weighting in equation xx. This demonstrates that the computed composite damping ratio for all the modes are erroneous since there is a degree of vibration of the steel girders

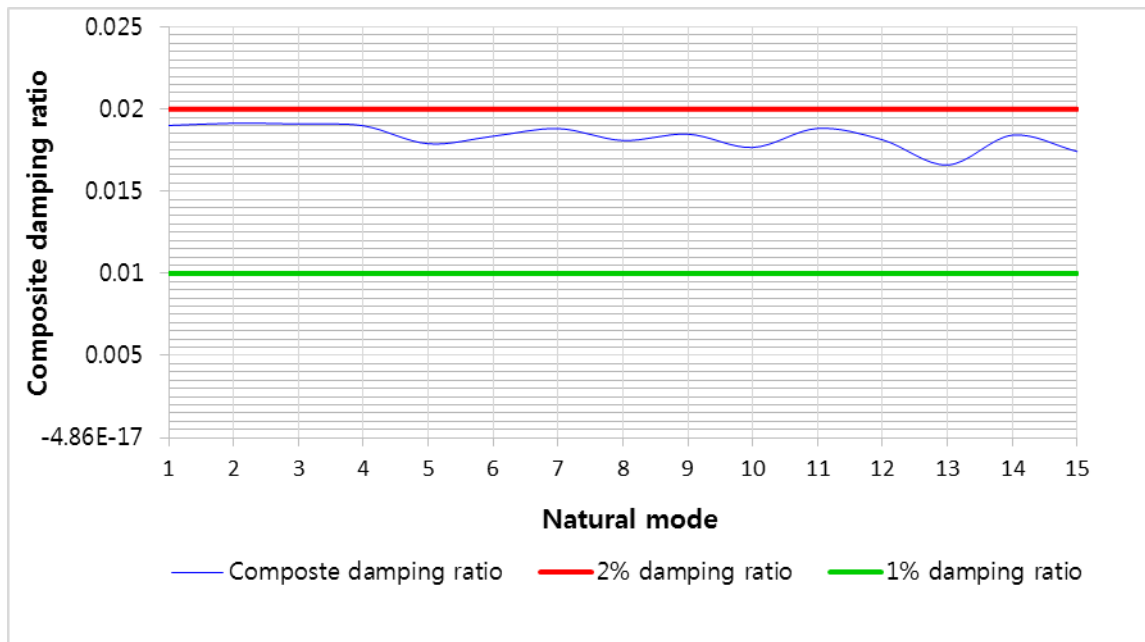


Fig. 12 Variation of composite damping ratio with increasing modes

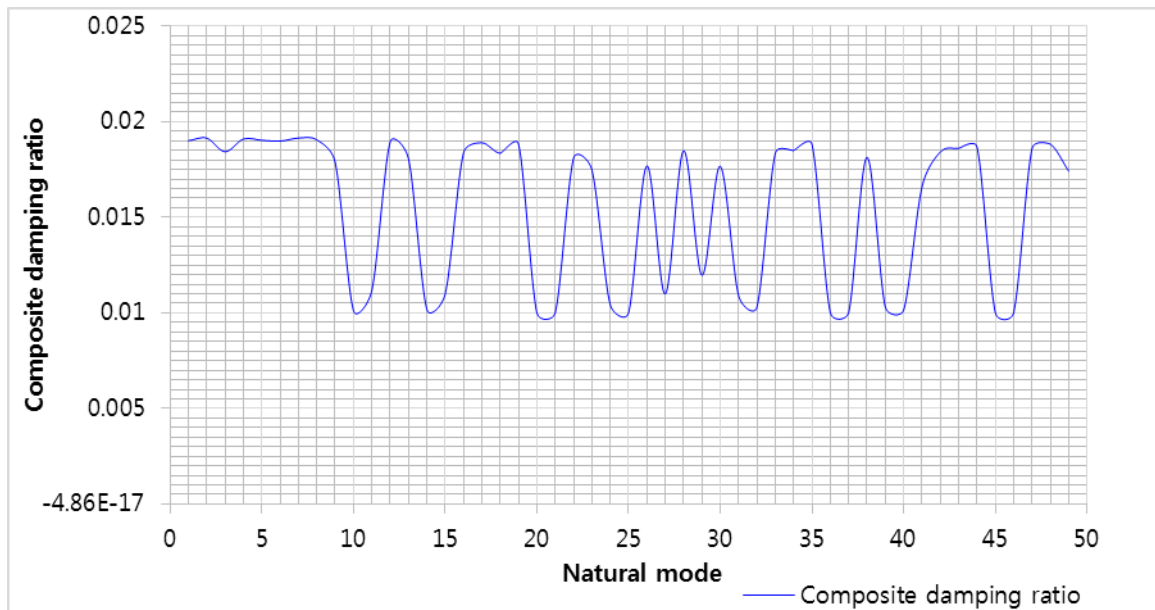


Fig. 13 Variation of composite damping ratio with increasing modes

coupled with the vibration of the slab panel for each mode due to the composite action between the two members of the deck.

Based on the above limitations, the validity of Dassault (2012) method was put in doubt and therefore not used further for the parametric study on variation of damping ratio.

5.5 Sensitivity of damping ratio

The study found that the effect of the variation of the uniform damping ratio on the natural frequencies of the slab panel was polynomial, based on Eq. (6) below adopted from Chopra (2011)

$$f_{nD} = f_n \sqrt{1 - \zeta_n^2} \tag{6}$$

Table 8 Percentage decrease in natural frequency for uniform damping ratios 1% to 5%

% decrease in natural frequency	Uniform damping ratio				
	1%	2%	3%	4%	5%
	0.005%	0.020%	0.045%	0.080%	0.125%

Based on Eq. (6), the % decrease in the natural frequency of the slab panel is as shown in Table 8 for the 1% to 5% uniform damping ratios. The percentage decrease at the high end of the parametric study range was regarded as very small to have any significant effect on the free vibration of the slab panel as suggested by Chopra (2011).

6. Conclusions

The fundamental undamped natural frequency of the slab panel was found to be 2.5981 Hz whilst the fundamental damped natural frequency was determined as 2.5976 Hz for a composite damping ratio of 1.901%. This fundamental damped natural frequency was found to be the same as the damped frequency calculated from a uniform 2% damping ratio. No significant difference was observed between the composite damping ratios computed by ABAQUS/Standard for all the modes and the uniform 2% damping ratio (based on the concrete material) used in the parametric study. This demonstrated that the composite damping ratio of the composite slab panel could be reasonably represented by a uniform material damping ratio based on the concrete material. Limitations were noted on Dassault (2012) method of computing the composite damping ratio. The fundamental natural mode shape was identified as transverse bending of the slab panel. A correlation of the natural frequencies of the slab panel with typical rail traffic frequency ranges showed that resonance damage from rail traffic vibration would likely result from transverse bending for low speed rail traffic, whilst this type of damage would likely result from both transverse bending and torsion for mid-high speed and high speed rail traffic. We have firstly observed that:

- The effect of variation of the concrete strength on the natural frequencies of the slab panel was found to be an increase in the natural frequencies with increasing strength of the concrete. An increase of 10.1% was observed in the fundamental natural frequency from increasing the concrete strength from 37 N/mm² to 115 N/mm², i.e., a 36.4% increase in the dynamic modulus of elasticity of the concrete.
- By varying the profiled steel sheeting stiffness, the effect on the natural frequencies of the slab panel was found to be an increase in the natural frequencies with increasing stiffness of the steel sheeting. An increase of 2.9% was observed in the fundamental natural frequency from increasing the modulus of elasticity from 50 KN/mm² to 215 KN/mm², i.e., a 330% increase in the modulus of elasticity of the steel.
- The effect of variation of the mass of concrete on the natural frequencies of the slab panel was found to be a decrease in the natural frequencies with increasing concrete

mass. Use of alternative deck sheeting materials (aluminium and carbon fibre sheeting) had the effect of lowering the fundamental natural frequency of the slab panel, however the differences were marginal among the three materials.

- By varying the uniform damping ratio of the slab panel, it was found out that the natural frequency decreased at a polynomial rate as the damping ratio increased.
- The crossover phenomenon observed during the parametric studies resulted in inversion of natural orders without interaction i.e., the modes retained their mode shapes before and after the crossover.

The concluding remarks made were that damping had marginal effect on the natural frequencies of the slab panel; varying the mass and stiffness changed the dynamic behaviour of the slab panel and subject to further studies, replacing the steel sheeting with aluminium or carbon fibre would have little effect on the dynamic behaviour of the slab panel. Future studies include the vibration behaviour of a steel-concrete composite slab panel for different track supports and fastening systems.

Acknowledgments

Technical assistance and support from Dr Olivia Mirza and Dane Griffin is highly appreciated. The first author would like to gratefully acknowledge the University of Birmingham's BRIDGE Grant, which financially supports his visiting professorship as part of the project "Improving damping and dynamic resistance in concrete through micro- and nano-engineering for sustainable and environmental-friendly applications in railway and other civil construction". This project is part of a collaborative BRIDGE program between the University of Birmingham and the University of Illinois at Urbana Champaign. He also wishes to thank the Australian Academy of Science and the Japan Society for the Promotion of Sciences for his Invitation Research Fellowship (Long-term) at the Railway Technical Research Institute and The University of Tokyo, Japan. In addition, the authors are sincerely grateful to the European Commission for the financial sponsorship of the H2020-RISE Project No. 691135 "RISEN: Rail Infrastructure Systems Engineering Network", which enables a global research network that tackles the grand challenges (Kaewunruen *et al.* 2016) of railway infrastructure resilience and advanced sensing in extreme environments (www.risen2rail.eu).

References

- ACP Composites (2016), High modulus carbon fibre. Available at: <http://www.acpsales.com/home.html> (Accessed on 1st July

- 2016).
- Benedettini, F., Zulli, D. and Allagio, R. (2009), "Frequency-veering and mode hybridization in arch bridges", *Proceedings of the IMAC-XXVII*, February 9-12 Orlando, Florida USA.
- Bezin, Y. and Farrington, D. (2010), "A structural study of an innovative steel-concrete track structure", *Proc. Inst. Mech. Eng. Part F: J. Rail Rapid Transit.*, **224**, 245-257.
- Bradford, M. and Uy, B. (2007), "Composite action of structural steel beams and precast concrete slabs for the flexural strength limit state", *Aust. J. Struct. Eng.*, **7**(2), 123-133.
- Britpave (2016), Why slab track. Available at: <http://www.britpave.org.uk/RailWhyBuild.ink> (Accessed: 9th July 2016).
- British Standards Institution (2002), BS EN 1991-1-1:2002 Eurocode 1-Actions on structures – Part 1-1: general actions – densities, self-weight, imposed loads for buildings. London: BSI.
- British Standards Institution (2004), BS EN 1992-1-1:2004 Eurocode 2- Design of concrete structures – Part 1-1: general rules and rules for buildings. London: BSI.
- British Standards Institution (2005), BS EN 1993-1-1:2005 Eurocode 3 – Design of steel structures – Part 1-1: general rules and rules for buildings. London: BSI.
- British Standards Institution (2000), BS EN 206-1:2000 Concrete – Part 1: specification, performance, production and conformity. London: BSI.
- British Standards Institution (1994), BS 5950-4:1994 Structural use of steelwork in building – Part 4: code of practice for design of composite slabs with profiled sheeting. London: BSI.
- British Standards Institution (1995), BS 5950-6:1995 Structural use of steelwork in building Part 6: code of practice for design of light gauge profiled steel sheeting. London: BSI.
- Choi, J.Y., Park, Y.G., Choi, E.S. and Choi, J.H. (2010), "Applying precast slab panel track to replace timber track in an existing steel plate girder railway bridge", *Proc. Inst. Mech. Eng. Part F: J. Rail Rapid Transit.*, **224**.
- Chopra, A.K. (2011), "Dynamics of structures – theory and applications to earthquake engineering", 4th Ed., Upper Saddle River, NJ: Prentice Hall. Prentice-Hall International Series in Civil Engineering and Engineering.
- Dassault (2012), ABAQUS theory manual. Available at: https://things.maths.cam.ac.uk/computing/software/abaqus_docs/docs/v6.12/books/stm/default.htm (Accessed on 1st August 2016).
- De Silva, S. and Thambiratnam, D.P. (2011), "Vibration characteristics of concrete-steel composite floor structures", *ACI Struct. J.*, **108**(6), 1-9.
- El-Dardiry, E. and Ji, T. (2006), "Modelling of the dynamic behaviour of profiled composite floors", *Eng. Struct.*, **28**(4), 567-579.
- Esveld, C. (1997), Low-maintenance ballastless track structures, Rail Engineering International Edition, No.3, 13-16.
- Feldmann, M., Heinemeyer, C., Butz, C., Caetano, E., Cunha, A., Galanti, F., Goldack, A., Hechler, O. Hicks, S., Keil, A., Lukic, M., Obiala, R., Schlaich, M., Sedlacek, G., Smith, A. and Waarts, P. (2009), Design of floor structures for human induced vibrations. Luxembourg: Office of the official publications of the European Communities.
- Freudenstein, S. (2010), "RHEDA 2000®: ballastless track systems for high-speed rail applications", *Int. J. Pavement Eng.*, **11**(4), 293-300.
- Griffin, D.W.P. (2013), Design of precast concrete steel-concrete panels for track support: for use on the Sydney Harbour Bridge, Honour Thesis, University of Western Sydney, Kingswood, Australia.
- Griffin, D.W.P., Mirza, O., Kwok, K. and Kaewunruen, S. (2014), "Composite slabs for railway construction and maintenance: a mechanistic review", *IES J. Part A: Civil. Struct. Eng.*, **7**(4), 243-262. doi: 10.1080/19373260.2014.947909
- Griffin, D.W.P., Mirza, O., Kwok, K. and Kaewunruen, S. (2015), "Finite element modelling of modular precast composites for railway track support structure: A battle to save Sydney Harbour Bridge", *Aust. J. Struct. Eng.*, **16**(2), 150-168. doi: 10.1080/13287982.2015.11465187
- Kaewunruen, S. (2014), "Monitoring in-service performance of fibre-reinforced foamed urethane material as timber-replacement sleepers/bearers in railway urban turnout systems", *Struct. Monit. Maint.*, **1**(1), 131-157 (invited). doi: 10.12989/smm.2014.1.1.131
- Kaewunruen, S. and Remennikov, A.M. (2007), "Field trials for dynamic characteristics of railway track and its components using impact excitation technique", *NDT & E Int.*, **40**(7), 510-519. doi: 10.1016/j.ndteint.2007.03.004
- Kaewunruen, S. and Remennikov, A.M. (2016), "Current state of practice in railway track vibration isolation: an Australian overview", *Aust. J. Struct. Eng.*, **14**(1), 63-71. doi: 10.1080/14488353.2015.1116364
- Kaewunruen, S., Remennikov, A.M. and Murray, M.H. (2014), "Introducing limit states design concept to concrete sleepers: an Australian experience", *Front. Mat.*, **1**(8), 1-3. doi: 10.3389/fmats.2014.00008
- Kaewunruen, S., Sussman, J.M. and Matsumoto, A. (2016), "Grand challenges in transportation and transit systems", *Front. Built Environ.*, **2**(4), doi: 10.3389/fbuil.2016.00004.
- Kim, H.Y. and Jeong, Y.J. (2006), "Experimental investigation on behaviour of steel-concrete composite bridge decks with perfo-bond ribs", *J. Constr. Steel Res.*, **62**, 463-471.
- Kim, H.Y. and Jeong, Y.J. (2009), "Steel-concrete composite bridge deck slab with profiled sheeting", *J. Constr. Steel Res.*, **65**, 1751-1762.
- Kim, H.Y. and Jeong, Y.J. (2010), "Ultimate strength of a steel concrete composite bridge deck slab with profiled sheeting", *Eng. Struct.*, **32**, 534-546.
- Kimani, S.K. and Kaewunruen, S. (2017), "Free vibrations of precast modular steel-concrete composite railway track slabs", *Steel Compos. Struct.*, **24**(1), 113-128. doi: 10.12989/scs.2017.24.1.113
- Lam, D. and El-Lobody, E. (2001), "Finite element modelling of headed stud shear connectors in steel-concrete composite beam", (Ed., A. Zingoni), *Struct. Eng. Mech. Compos.*, Elsevier Science, Oxford, 401-408.
- Lezgy-Nazargah, M. and Kafi, L. (2015), "Analysis of composite steel-concrete beams using a refined high-order beam theory", *Steel Compos. Struct.*, **18**(6), 1369-1389.
- Manalo, A., Aravinthan, T., Karunasena, W. and Ticoalu, A. (2010), "A review of alternative materials for replacing existing timber sleepers", *Compos. Struct.*, **92**, 603-611.
- Matias, S. (2015), Numerical modelling and design of slab tracks - comparison with ballasted tracks, University of Lisbon.
- Max Bogl (2016), FFB slab track BOGL. Available at: <https://max-boegl.de/en> (Accessed on 1st July 2016)
- Mello, A.V.de A., da Silva, J.G.S., Vellasco, P.C.G.da S., de Andrade, S.A.L. and de Lima, L.R.O. (2008), "Modal analysis of orthotropic composite floors slabs with profiled steel decks", *Lat. Am. J. Solids Struct.*, **5**(1).
- Michas, G. (2012), Slab track systems for high-speed railways, Master Degree Project, Royal Institute of Technology, Sweden.
- Mirza, O., Kaewunruen, S., Kwok, K. and Giffins, D. (2016), "Design and modelling of pre-cast steel-concrete composites for resilient railway track slabs", *Steel Compos. Struct.*, **22**(3), 537-565. doi: 10.12989/scs.2016.22.3.537
- Peng, D., Wei, Z. and Liu, J. (2012), "The exploration and research of CRTS I slab ballastless track used in the freight lines", *Appl. Mech. Mater.*, **253-255**, 2031-2034.
- Perkins, N.C. and Mote, Jr. (1986), "Comments on curve veering

- in eigenvalue problems”, *J. Sound Vib.*, **106**(3), 451-463.
- Remennikov, A.M. and Kaewunruen, S. (2008), “A review of loading conditions for railway track structures due to train and track vertical interaction”, *Struct. Control Health Monit.*, **15**(2), 207-234. doi: 10.1002/stc.227
- Remennikov, A.M., Murray, M.H. and Kaewunruen, S. (2012), “Reliability based conversion of a structural design code for prestressed concrete sleepers”, *Proc. Inst. Mech. Eng. : Part F J. Rail. Rapid Transit*, **226**(2), 155-173. doi: 10.1177/0954409711418754
- Remennikov, A.M. and Kaewunruen, S. (2014), “Experimental load rating of aged railway concrete sleepers”, *Eng. Struct.*, **76**(10), 147-162. doi: 10.1016/j.engstruct.2014.06.032
- Robertson, I., Masson, C., Sedran, T., Barresi, F., Caillau, J., Keseljevic, C. and Vanzenberg, J.M. (2015), “Advantages of a new ballastless track form”, *Constr. Build. Mater.*, **92**, 16-22.
- Setsobhonkul, S., Kaewunruen, S. and Sussman, J.M. (2017), “Lifecycle assessments of railway bridge transitions exposed to extreme climate events”, *Front. Built Environ.*, **3**(35), doi: 10.3389/fbuil.2017.00035.
- Shim, C.S., Lee, P.G. and Chang, S.P. (2001), “Design of shear connection in composite steel and concrete bridges with precast decks”, *J. Constr. Steel Res.*, **57**, 203-219.
- Smith, A.L., Hicks, S.J. and Devine, P.J. (2009), “Design of floors for vibration: a new approach”, Ascot: The Steel Construction Institute.
- Sugimoto, I., Yoshida, Y. and Tanikaga, A. (2013), “Development of composite steel girder and concrete slab method for renovations of existing steel railway bridges”, *QR of RTRI*, **54**(1), 1-11.
- Tindall, P. (2008), “Aluminium in bridges”, (Eds., Parke, G and Hewson, N.) ICE manual of bridge engineering, 2nd Ed., London: Thomas Telford, 345- 355.
- Tuler, M.V. and Kaewunruen S. (2017), “Life cycle analysis of mitigation methodologies for railway rolling noise and groundbourne vibration”, *J. Environ. Management*, **191**, 75-82. doi: 10.1016/j.jenvman.2016.12.075
- Venghiac, V.M. and D’Mello, C. (2010), The influence of the thickness of the slab and concrete grade on composite floors, *Buletinul Institutului Politehnic Din Iasi*.